Chalcogenide Letters Vol. 21, No. 4, April 2024, p. 335 - 342

Facile hydrothermal synthesis of a multifunctional copper zinc tin sulfide (CZTS) nanoparticle-coated sepiolite fiber composite: structural characterization and photocatalytic properties

M. Boonkam, P. Tamdee, P. Tongying*
Department of Chemistry, Faculty of Science, Silpakorn University, Nakhon Pathom, Thailand 73000

This work presents a facile hydrothermal synthesis method for fabricating a multifunctional composite of copper zinc tin sulfide (CZTS) nanoparticles coated onto sepiolite fibers. Morphological analysis confirms the firm attachment of approximately 10 nm CZTS nanoparticles onto the sepiolite surface. Elemental analysis verifies the presence of constituent elements from both CZTS and sepiolite, with a slight deficiency in Cu and an abundance of Zn observed. The compositional formula of CZTS in the composite is estimated as $Cu_{1.93}Zn_{1.05}Sn_{0.98}S_{4.04}$. Notably, the material exhibits a narrow band gap of 1.5 eV, enabling effective utilization of the entire visible light spectrum, making it promising for photocatalytic applications. BET nitrogen adsorption/desorption measurements reveal a substantial surface area of approximately 85.720 m^2/g, confirming the composite's versatility and applicability, particularly in photocatalysis and adsorption processes. Additionally, X-ray diffraction analysis indicates reflections consistent with the crystal structures of kasterite CZTS and sepiolite, further confirming the composite's composition. The multifunctional CZTS/Sepiolite composite demonstrates exceptional potential for simultaneous photocatalytic degradation and adsorption of organic pollutants, presenting a promising avenue for sustainable water treatment applications.

(Received February 14, 2024; Accepted April 23, 2024)

Keywords: CZTS/Sepiolite, CZTS nanoparticles, Sepiolite, Hydrothermal synthesis

1. Introduction

Photocatalysis, a method capable of decomposing diverse organic compounds, holds significant promise for water treatment applications. This technique relies on photocatalysts, primarily semiconductor materials such as ZnO, WO_3, and TiO_2 [1-3]. However, despite TiO_2's extensive study due to its specific physical and chemical properties and relatively low production cost, it exhibits limitations in light response, especially in the ultraviolet (UV) range (E_g ~3.2 eV). Addressing the limited UV light proportion in the solar spectrum compared to visible light, the development of photocatalysts capable of visible light absorption remains imperative for practical applications. Semiconductor materials like copper zinc tin sulfide (CZTS or Cu_2ZnSnS_4), characterized by a relatively narrow direct band gap (E_g ~1.5 eV) and high absorption coefficient (10^4 cm^{-1}) [4, 5], hold promise as light-absorbing photocatalysts for contaminant degradation. It is one of the most promising absorber materials in earth abundant, non-toxic, cost-effective solar cell thin films [6, 7]. It has been reported that the photovoltaic device fabricated from the absorber CZTS exhibit the conversion efficiency reaching 11% [8].

Sepiolite, a microfibrous clay mineral, is distinguished by its layered structure comprising two tetrahedral silica sheets and a central magnesia sheet [9]. This unique configuration forms structural tunnels that contribute to its intriguing surface properties and notable adsorption capacity [10]. The micro-fibrous arrangement results in a significant porous volume and a specific surface area exceeding 300 m^2/g [11], facilitating robust adsorption of organic substances. For example, the dispersion of photocatalysts like TiO_2 and ZnO onto sepiolite has been demonstrated to enhance their photocatalytic efficiency [12, 13]. Consequently, sepiolite holds promise as a supportive

* Corresponding author: tongying_p@su.ac.th
https://doi.org/10.15251/CL.2024.214.335

material for CZTS catalysts, potentially enhancing their adsorption capacity and improving their photocatalytic performance.

This study aims to develop a versatile CZTS/Sepiolite composite material, designed to function both as an adsorbent and a photocatalyst, utilizing a straightforward hydrothermal synthesis approach. This composite integrates sepiolite—an abundant, cost-effective mineral possessing a fibrous structure for adsorption purposes—with CZTS nanoparticles serving as the photocatalyst. Our objectives include estimating the compositional formula of CZTS in the composite, investigating its band gap energy, and assessing its specific surface area suitability for efficient operation within the visible spectrum.

2. Experimental

2.1. Chemicals and materials

Zinc chloride anhydrous ($ZnCl_2$) and ethylene glycol (1,2-ethanediol) were acquired from Carlo Erba reagents. Tin (II) chloride ($SnCl_2$, anhydrous) was obtained from Merck KGaA. Copper (II) chloride anhydrous ($CuCl_2$, analysis grade) was purchased from Alfa Aesar. Thiourea (NH_2CSNH_2, AR grade) was sourced from LOBA Chemie Pvt. Ltd. Oleic acid ($C_{18}H_{34}O_2$, technical grade) and sepiolite powder (technical grade) were purchased from Sigma-Aldrich. Ethyl alcohol (99.99%, AR grade) was obtained from QReC New Zealand.

2.2. Preparation of CZTS/Sepiolite composites

The CZTS/Sepiolite composites were prepared through a hydrothermal process, with oleic acid employed as a surfactant [14]. $CuCl_2$, $ZnCl_2$, $SnCl_2$, and thiourea were dissolved in 100 ml of ethylene glycol in the appropriate proportions, using a Cu:Zn:Sn:S molar ratio of 2:1:1:4. The mixture was thoroughly stirred. Following this, 3.0 ml of oleic acid was added and mixed until a uniform blend was achieved. Next, sepiolite powder in varying amounts (2 and 4 g) was introduced, and stirring continued until a homogeneous mixture was obtained. The resulting mixture was then transferred to a Teflon-lined stainless-steel autoclave, which was subsequently placed in an oven and heated to 200 ℃, where it remained for 18 hours. Subsequently, it was permitted to cool to room temperature. The resultant product was isolated from the solution via centrifugation and subjected to multiple washes with ethanol until the solution above the precipitate clarified. Ultimately, the resultant product underwent oven-drying at 80 ℃ for 24 hours. The synthesis of CZTS nanoparticles followed the same procedure as used for preparing CZTS/Sepiolite composites, without the addition of sepiolite.

2.3. Materials characterization

The surface characteristics of both the pure sepiolite and the CZTS/Sepiolite composite samples were analyzed using a TESCAN MIRA-3 FE-SEM system. Additionally, EDS analysis was carried out using the same TESCAN MIRA-3 FE-SEM system, equipped with an Oxford detector. The surface area according to Brunauer-Emmett-Teller (BET) and the distribution of pore sizes were determined utilizing a Quantachrome instrument.

For XRD analysis, a PANalytical Aeris X-Ray diffractometer was employed, covering the 2θ range of 5-65 degrees. Cu Kα radiation at 40 kV and 8 mA was utilized for this analysis. The average CZTS crystallite size was determined using the Debye-Scherrer equation, $D = K\lambda/\beta\cos\theta$, where D was used to represent the average crystal diameter. This calculation involved various factors, including the corrected peak width (referred to as β), a constant associated with crystallite shape (K, with a value of 0.9), the wavelength of X-rays used (λ), and the diffraction angle (θ). The specific focus of this calculation was on the width of the diffraction peak that displayed the highest intensity.

For UV-visible diffuse reflectance spectra (UV-Vis DRS) analysis, a Shimadzu UV-2600i spectrophotometer operated at room temperature under ambient atmospheric conditions was used. The reflectance spectrum was captured within the wavelength range of 200-1300 nm. To determine the band gap (E_g) for both the CZTS/Sepiolite composite samples and the pure CZTS nanoparticles, the Kubelka-Munk function was applied [15]. This function is represented as $F(R_\infty) = (1 –$

$R_\infty)^2/(2R_\infty)$, where R_∞ was computed as R_{sample}/R_{ref}, reflecting the reflectance intensity of a specimen with infinite thickness, utilizing $BaSO_4$ as a reference. The band gap (E_g) was determined by identifying the intersection point of the x-axis with the linear extrapolation of the graph in the corresponding Tauc plots ($[F(R_\infty)\times h\nu]^{1/\gamma}$ versus photon energy ($h\nu$)) [16]. It's noteworthy that, in this scenario, the value of γ is 1/2, given that CZTS is considered as a direct band gap semiconductor [17].

3. Results and discussions

The morphological characteristics of pure sepiolite, synthesized CZTS nanoparticles, and CZTS/Sepiolite composites were examined using SEM. As shown in Fig. 1a, pure sepiolite exhibits a fibrous structure with an average diameter of approximately 50 nm and variable lengths ranging from several hundred nanometers to several micrometers. Fig. 1c and 1d reveal CZTS nanoparticles on the surface of the sepiolite, indicating that the CZTS nanoparticles were successfully synthesized and loaded onto the sepiolite without altering the original surface morphology. The particle size of CZTS in CZTS/Sepiolite is approximately 10 nm, which agrees with the size of the synthesized CZTS nanoparticles without the addition of sepiolite (see Fig. 1b).

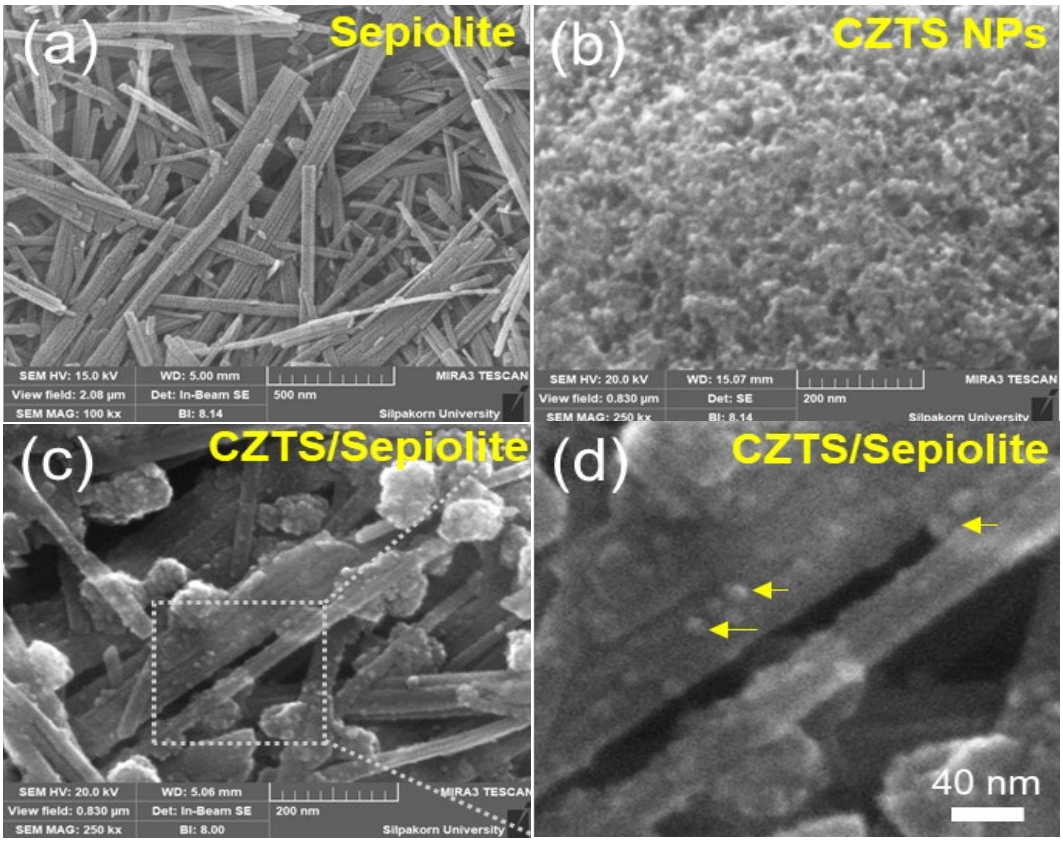

Fig. 1 SEM images of pure sepiolite (a), CZTS nanoparticles (b), and CZTS/Sepiolite(2 g) (c and d). Arrows in (d) indicate the CZTS nanoparticles attached to the surface of the fibrous-structured sepiolite.

Elemental analysis was conducted to investigate the elemental composition of the synthesized CZTS/Sepiolite composite, CZTS nanoparticles, and sepiolite. Fig. 2a displays the EDS spectrum obtained from the CZTS/Sepiolite composite containing 2 g of sepiolite. The spectrum exhibits distinct peaks corresponding to the constituent elements, including Cu, Zn, Sn, and S originating from CZTS (Fig. 2b), as well as Si and Mg, both deriving from sepiolite (Fig. 2c). The

CZTS/Sepiolite composite sample reveals a slight deficiency in Cu and an abundance of Zn, evidenced by its Cu/(Zn + Sn) ratio of 0.95 and a Zn/Sn ratio of 1.06. This observation is similar to the findings from the synthesized CZTS nanoparticles sample [18, 19]. Previous studies have indicated that nonstoichiometric CZTS compositions, with Cu/(Zn + Sn) ratios ranging from 0.75 to 1 and Zn/Sn ratios between 1 and 1.25 [20-23], demonstrate remarkable solar cell conversion efficiencies reaching 11% [8]. Based on the EDS analysis, the compositional formula is estimated as $Cu_{1.93}Zn_{1.05}Sn_{0.98}S_{4.04}$/Sepiolite composite, meeting the criteria of an effective absorber material.

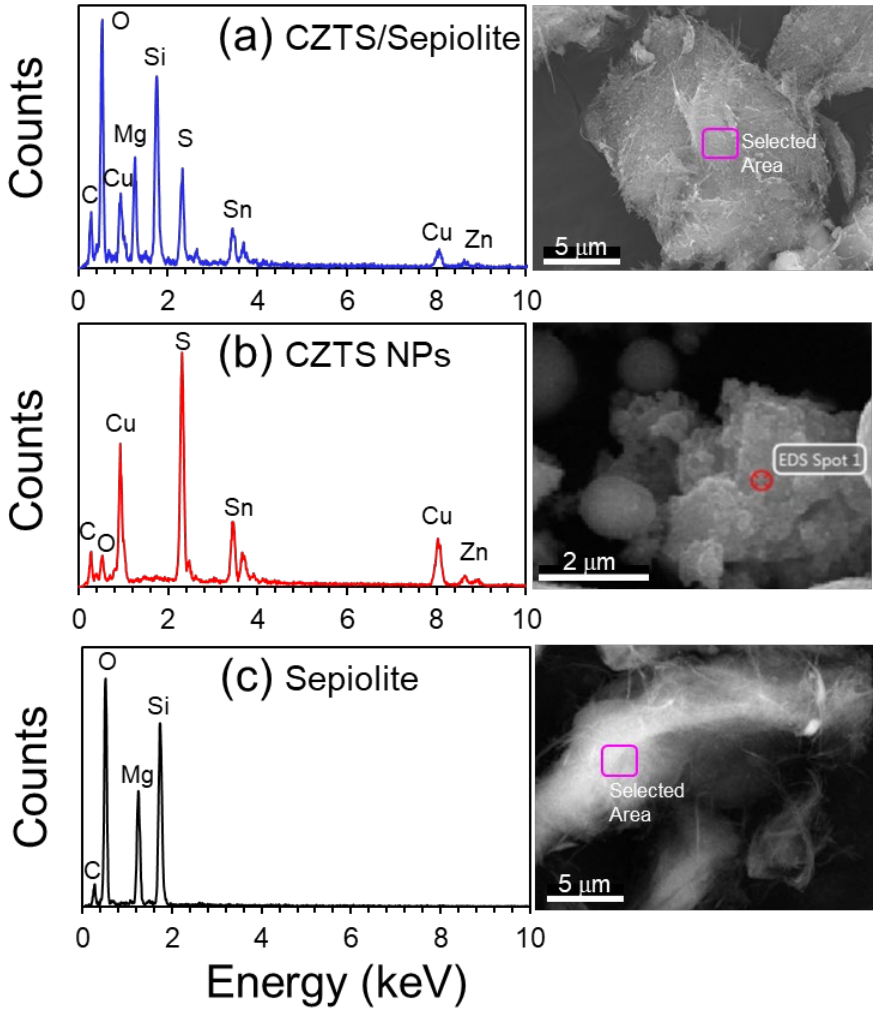

	CZTS	CZTS/Sepiolite
Cu (at%)	24.5 ± 2.3	24.1 ± 0.8
Zn (at%)	13.4 ± 0.6	13.1 ± 2.2
Sn (at%)	12.5 ± 0.8	12.3 ± 1.2
S (at%)	49.5 ± 3.6	50.5 ± 1.2
Cu/(Zn+Sn)	0.95	0.95
Zn/Sn	1.07	1.06

Fig. 2 The EDS spectra of (a) CZTS/Sepiolite composite (2 g), (b) CZTS nanoparticles, and (c) pure sepiolite were obtained from the spots indicated in the corresponding SEM images.

X-ray diffraction analysis was conducted to investigate the crystal structure of the prepared materials. As depicted in Fig. 3, the composition and structure of CZTS/Sepiolite composite materials were identified through XRD spectra and agree with kesterite CZTS and sepiolite. The reflections observed at 2θ angles of 28.46°, 47.38°, and 56.14°, corresponding to the (112), (220), and (312) lattice planes of kesterite CZTS, were in accordance with JCPDS Card No. 26-0575. Additionally, reflections at 2θ angles of 7.38°, 20.63°, and 35.04°, associated with the (110), (131), and (371) lattice planes of sepiolite, matched well with PDF Card No.13-0595. It's worth noting that the intensity of the reflection peaks of sepiolite increased as the amount of sepiolite increased from 2 g to 4 g. The crystallite size of CZTS in CZTS/Sepiolite composite samples containing 2 g and 4 g of sepiolite was calculated using the Scherrer equation, resulting in values of approximately 10.7 nm and 9.6 nm, respectively, which closely resemble the particle size of CZTS (10.7 nm). The crystallite size calculated from the XRD pattern agrees well with SEM images (Fig. 1b, c, d).

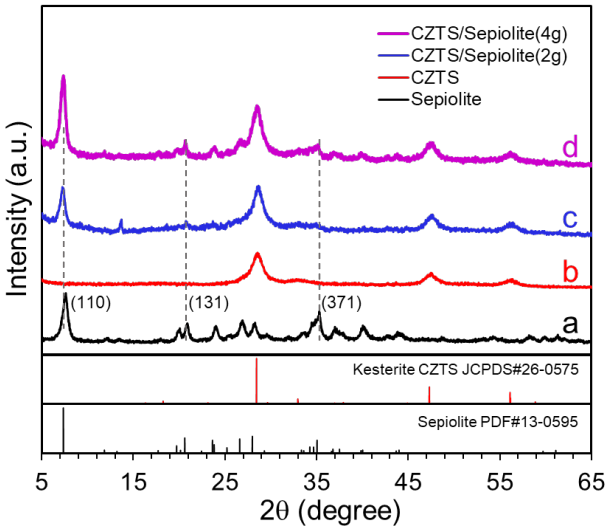

Fig. 3. XRD patterns of pure sepiolite (a), CZTS nanoparticles (b), and CZTS/Sepiolite composites containing 2 g (c) and 4 g (d) of sepiolite.

Fig. 4a presents the UV-vis diffuse reflectance (DRS) spectra of pure sepiolite, synthesized CZTS nanoparticles, and the CZTS/Sepiolite composites. The DRS spectrum of pure sepiolite exhibits a characteristic wide band gap property, with an absorption edge at approximately 250 nm. This indicates limited optical response to visible light. CZTS/Sepiolite samples with 2 and 4 g of sepiolite display absorption edges that extend into the 800 nm range, aligning with the intrinsic light absorption properties of CZTS [4]. This illustrates the capability of the composites to absorb light across the entire visible region.

The optical band gap of CZTS/Sepiolite composite samples and CZTS nanoparticles was determined from the diffuse reflection spectrum using the Kubelka-Munk function. Tauc plots, represented by $(F(R\infty)\times h\nu)^2$ versus photon energy ($h\nu$), are displayed in Fig. 4b.

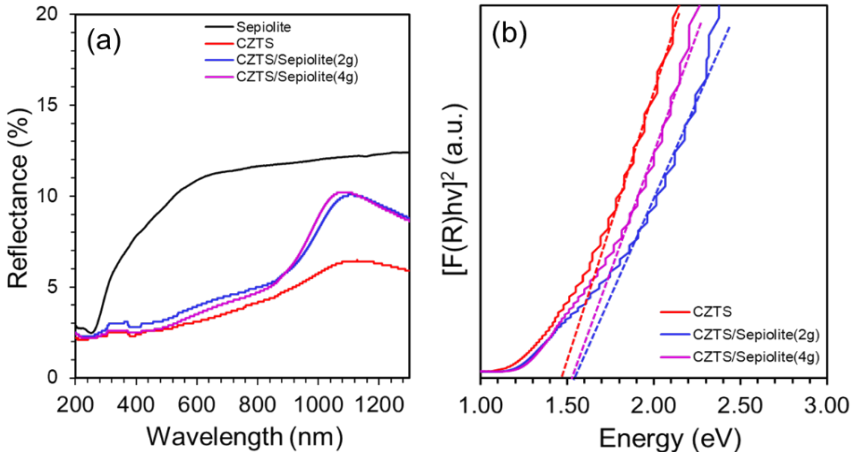

Fig. 4. (a) UV-vis diffuse reflectance spectra of sepiolite, synthesized CZTS nanoparticles, and CZTS/Sepiolite composites with varying amounts of sepiolite (2 and 4 g). (b) Graphs depicting the transformed Kubelka-Munk function plotted against photon energy for both CZTS nanoparticles and CZTS/Sepiolite composites.

The intersection of the linear fit with the photon energy axis yields the band gap values, which were measured as 1.53 and 1.52 eV for the CZTS/Sepiolite(2g) and CZTS/Sepiolite(4g), respectively. These determined band gap values for CZTS/Sepiolite composites agrees well with the estimated band gap of CZTS nanoparticles which is 1.48 eV. The observed band gap closely matches the range reported in the literature, which is between 1.4 and 1.5 eV [4, 24-26]. This result highlights the substantial promise of this composite material for diverse photocatalytic applications, as it demonstrates the ability to capture light across the entire visible spectrum.

The surface area is a crucial parameter for adsorbents, as it directly influences the adsorption capacity of a material towards an adsorbate. In this study, we conducted BET nitrogen adsorption and desorption measurements at 77 K to evaluate the surface area and pore characteristics of the CZTS/Sepiolite composite sample. According to the IUPAC classification, the CZTS/Sepiolite composite containing 2 g of sepiolite exhibited a Type V isotherm shape (see Fig. 5a) [27]. The specific surface area of the CZTS/Sepiolite composite is 85.720 m^2/g, which is approximately twice larger than that of CZTS nanoparticles alone (44.659 m^2/g). The pore volume and average pore diameter of the CZTS/Sepiolite(2g) composite during the adsorption and desorption process are 0.353 cm^3/g and 7.032 nm, respectively (Fig. 5b).

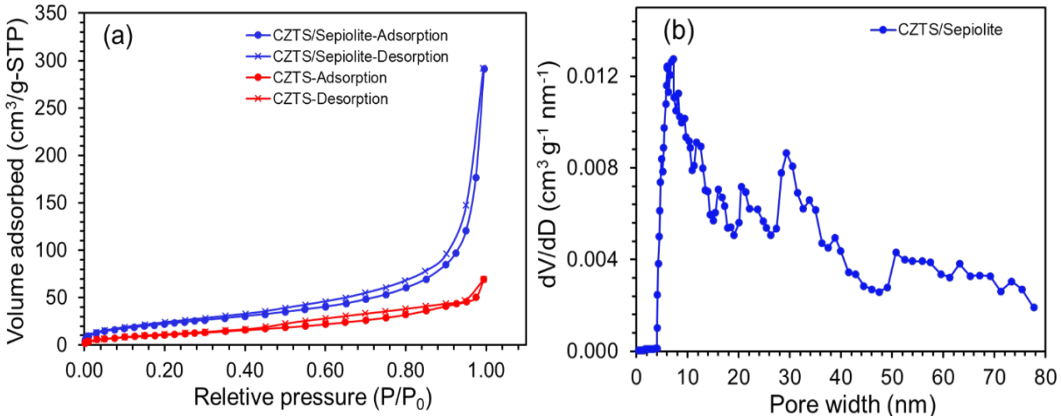

Fig. 5. (a) Nitrogen adsorption-desorption isotherm at 77 K of CZTS nanoparticles and CZTS/Sepiolite (2 g) composite. (b) Pore size distribution of CZTS/Sepiolite (2 g) composite.

4. Conclusions

In summary, our study effectively employed a facile hydrothermal method to coat sepiolite fibers with CZTS nanoparticles. Morphological analysis unveiled firmly attached CZTS nanoparticles, approximately 10 nm in size, onto the sepiolite surface. Elemental analysis confirmed the presence of constituent elements from both CZTS and sepiolite. The composite displayed a slight deficiency in Cu and an abundance of Zn, indicated by its Cu/(Zn + Sn) ratio of 0.95 and Zn/Sn ratio of 1.06. The compositional formula of CZTS in the composite was estimated as $Cu_{1.93}Zn_{1.05}Sn_{0.98}S_{4.04}$.

Notably, the material exhibited a narrow band gap (1.52 and 1.53 eV), enabling effective utilization of the entire visible light spectrum, showing promise in various applications, particularly in the field of photocatalysis. BET nitrogen adsorption and desorption measurements revealed a substantial surface area of approximately 85.720 m^2/g, confirming the versatility and applicability of the CZTS/Sepiolite composite, particularly in photocatalysis and adsorption applications.

Acknowledgements

The authors are grateful for the financial support received from the New Researcher Scholarship of CSTS, MOST; the Coordinating Center for Thai Government Science and Technology Scholarship Students (CSTS); the National Science and Technology Development Agency-NSTDA, Thailand (Project no.: JRA-CO-2564-14885-TH); and the Faculty of Science, Silpakorn University, Thailand (Project no.: SRIF-JRG-2566-18).

References

[1] S.J. Armaković, M.M. Savanović, S. Armaković, Catalysts, **13**(1), (2022); https://doi.org/10.3390/catal13010026
[2] Bharti, J. Jangwan, S.S. Kumar, V. Kumar, A. Kumar, D. Kumar, Appl Water Sci, **12**(3), (2022); https://doi.org/10.1007/s13201-021-01566-3
[3] P. Shandilya, S. Sambyal, R. Sharma, P. Mandyal, B. Fang, Journal of hazardous materials, **428**((2022); https://doi.org/10.1016/j.jhazmat.2022.128218
[4] H. Katagiri, K. Jimbo, W.S. Maw, K. Oishi, M. Yamazaki, H. Araki, A. Takeuchi, Thin Solid Films, **517**(7), 2455 (2009); https://doi.org/10.1016/j.tsf.2008.11.002
[5] J.-S. Seol, S.-Y. Lee, J.-C. Lee, H.-D. Nam, K.-H. Kim, Solar energy materials and solar cells, **75**(1-2), (2003); https://doi.org/10.1016/S0927-0248(02)00127-7
[6] P.D. Antunez, D.M. Bishop, Y. Luo, R. Haight, Nature Energy, **2**(11), 884 (2017);
[7] M.A. Green, Nature Energy, **1**(1), 15015 (2016); https://doi.org/10.1038/nenergy.2015.15
[8] C. Yan, J. Huang, K. Sun, S. Johnston, Y. Zhang, H. Sun, A. Pu, M. He, F. Liu, K. Eder, Nature energy, 3(9), 764 (2018); https://doi.org/10.1038/s41560-018-0206-0
[9] J. Valentín, M. López-Manchado, A. Rodríguez, P. Posadas, L. Ibarra, Applied Clay Science, **36**(4), (2007); https://doi.org/10.1016/j.clay.2006.10.005
[10] G. Zhang, Q. Xiong, W. Xu, S. Guo, Applied clay science, **102**((2014); https://doi.org/10.1016/j.clay.2014.10.001
[11] U. Shuali, S. Nir, G. Rytwo, Developments in Clay Science, Elsevier, 2011, pp. 351-374; https://doi.org/10.1016/B978-0-444-53607-5.00015-3
[12] F. Zhou, C. Yan, H. Wang, S. Zhou, S. Komarneni, Applied Clay Science, **146**((2017); https://doi.org/10.1016/j.clay.2017.06.010
[13] C. Li, H. Li, G. He, Z. Lei, W. Wu, Advances in materials science and engineering, **2021**((2021); https://doi.org/10.1155/2021/5357843
[14] M.Z. Ansari, M. Faraz, S. Munjal, V. Kumar, N. Khare, Advanced Powder Technology, **28**(9), 2402 (2017); http://dx.doi.org/10.1016/j.apt.2017.06.023
[15] P. Kubelka, F. Munk, Z. Tech. Phys, **12**(593), (1931)

[16] P. Makuła, M. Pacia, W. Macyk, The Journal of Physical Chemistry Letters, 9(23), (2018); https://doi.org/10.1021/acs.jpclett.8b02892
[17] S. Chen, A. Walsh, Y. Luo, J.-H. Yang, X. Gong, S.-H. Wei, Physical Review B, 82(19), 195203 (2010); https://doi.org/10.1103/PhysRevB.82.195203
[18] D. Xia, Y. Zheng, P. Lei, X. Zhao, Physics Procedia, **48**((2013); https://doi.org/10.1016/j.phpro.2013.07.036
[19] M. Khushaim, S. Alamri, N. Kattan, A. Jaber, S. Alamri, Journal of Taibah University for Science, **15**(1), (2021); https://doi.org/10.1080/16583655.2021.1978809
[20] S. Chen, A. Walsh, X.G. Gong, S.H. Wei, Advanced materials, **25**(11), (2013); https://doi.org/10.1002/adma.201203146
[21] W. Ki, H.W. Hillhouse, Advanced Energy Materials, **1**(5), (2011); https://doi.org/10.1002/aenm.201100140
[22] D.B. Mitzi, O. Gunawan, T.K. Todorov, K. Wang, S. Guha, Solar Energy Materials and Solar Cells, **95**(6), (2011); https://doi.org/10.1016/j.solmat.2010.11.028
[23] M. Courel, J. Andrade-Arvizu, A. Guillén-Cervantes, M. Nicolás-Marín, F. Pulgarín-Agudelo, O. Vigil-Galán, Materials & Design, **114**((2017); https://doi.org/10.1016/j.matdes.2016.10.068
[24] Q. Guo, H.W. Hillhouse, R. Agrawal, J Am Chem Soc, 131(33), (2009); https://doi.org/10.1021/ja904981r
[25] G. Tseberlidis, V. Trifiletti, E. Vitiello, A.H. Husien, L. Frioni, M. Da Lisca, J. Alvarez, M. Acciarri, S.O. Binetti, ACS Omega, 7(27), (2022); https://doi.org/10.1021/acsomega.2c01786
[26] S. Engberg, J. Symonowicz, J. Schou, S. Canulescu, K.M.Ø. Jensen, ACS Omega 5(18), (2020); https://doi.org/10.1021/acsomega.0c00657
[27] K.S. Sing, Pure and applied chemistry **57**(4), 603 (1985); https://doi.org/10.1351/pac198557040603